Combination of Multisatellite Altimetry and Tide Gauge Data for Determining Vertical Crustal Movements along Northern Mediterranean Coast

F. García,[1] M. I. Vigo,[1] D. García-García,[1] and J. M. Sánchez-Reales[1]

Abstract—Sea level variations (SLV) can be measured by tide gauges (TG) at the coast and by altimeters onboard satellites. The former measures the SLV relative to the coast, whereas altimetry provides the SLV with respect to a geocentric reference frame. The differences between SLV measurements from these two techniques can be used as an indirect assessment of vertical crustal motions at the TG sites. In this study, we exploit this idea, analyzing differences between sea level signals as measured by altimetric missions (TOPEX/Poseidon and Jason-1) and by 47 TG stations along northern Mediterranean coasts for the period 1993–2007. This allows us to estimate the vertical land motion along these coasts at the TG sites in this time window. For those sites where the TG is co-located or has a nearby global positioning system (GPS) station, these estimates are compared with the vertical rates derived from GPS measurements. Our results on vertical ground motion along the Mediterranean coast provide a useful source of data for studying, contrasting, and constraining tectonic models for the region.

Key words: Mediterranean Sea, sea level, altimetry, tide gauge, vertical crustal motion.

1. Introduction

Sea level variations (SLV) are primarily determined by two methods. For almost two centuries, the long-term SLV has been typically estimated from tide gauge (TG) measurements (e.g., BARNETT, 1984; DOUGLAS, 1991). Alternatively, during the last two decades, altimeters onboard satellites, whose orbits are precisely determined, have provided SLV measurements with high accuracy. Satellite altimeters measure SLV with respect to an ellipsoid of reference, whereas TG measurements are relative to the land on which the TG rests. By itself, a tide gauge cannot tell the difference between local crustal motion and sea level changes. However, the combination of the two techniques can provide information for estimating vertical crustal motions at the TG sites, which is complementary to and independent of global positioning system (GPS) measurements at these sites.

CAZENAVE *et al.* (1999) combined altimetry and TG data, for the period 1993–1997, to estimate the vertical ground motion at 53 TG sites, mainly located in the Pacific Ocean. The basic idea is to form the difference time series for altimetry minus TG, and examine its long-term behavior. This approach can provide information about the long-term vertical ground motion in the absolute sense. Six of these estimates were verified by Doppler orbitography and radio-position integrated by satellite (DORIS) data. A recent study by RAY *et al.* (2010), following the same idea but extending the study to a 16-year period (1993–2009), analyzed the vertical ground motion of 28 TG and compared the results with recent DORIS-derived vertical rates. The first estimations for the northern Mediterranean and Black Sea coasts, following a similar technique, are presented in GARCIA *et al.* (2007) with results corresponding to a 9-year period (1993–2001). Results for most areas are in accordance with the tectonic setting of the Mediterranean, which is dominated by subduction in the Hellenic and Calabrian Arc and by the collision between the African and Arabian Plates with Eurasia, but with several regions of extension, such as the Alboran Sea, the Algero-Provencal Basin, and the Tyrrhenian and Aegean Seas (JIMENEZ-MUNT *et al.*, 2003). The tectonic-seismic activity is higher in the eastern Mediterranean and becomes quieter towards the north.

[1] Departamento de Matemática Aplicada, Escuela Politécnica Superior, Universidad de Alicante, San Vicente del Raspeig, 03080 Alicante, Spain. E-mail: Fernando.GC@ua.es

Furthermore, the results also provide significant information for other areas, such as the distinct land subsidence on the west coast of Greece and the east coast of the Adriatic Sea, which can constitute an indicator that may be related to the Adriatic lithosphere subduction beneath the Eurasian Plate along the Dinarides Fault (BENNETT et al. 2008). However, though the main contribution to the vertical land motion here reported should be tectonic, there can be other anthropogenic origins that might be dominant at specific locations.

In this study, we revisit the problem presented in GARCIA et al. (2007), but the approach here presented has been significantly improved in several aspects: (1) the time period has been extended in most cases up to 15 years (1993–2007); (2) the altimetric measurements used have been improved near the coast; and (3) in order to make both data types as consistent as possible, TG measurements are corrected for ocean, atmospheric, and hydrological loading, and for the ocean pole tide. Besides, the glacial isostatic adjustment (GIA) has been corrected following PELTIER (2004); although the vertical displacement produced at the Mediterranean coast by the GIA is minimal, it can represent a significant portion of the observed vertical rate at some specific sites (STOCCHI and SPADA, 2009).

2. Data

2.1. Altimetry Data

The altimetry data used in this study are along track measurements from TOPEX/Poseidon (T/P) and Jason-1. Altimetry was originally designed for the open ocean, and the quality of altimetric measurements decreases in proximity to the coast, where our interest lies. However, in recent years, great improvement of satellite altimetry quality in the coastal zones has been achieved by the development of data products specially processed for coastal applications. In this work we use altimetry sea level anomalies from a regional solution for the Mediterranean Sea which is part of the coastal products developed, validated, and distributed by the Centre de Topographie des Océans et de l'Hydrosphère (CTOH) in France. The altimetric

measurements are based on the round trip of a radar pulse between the satellite and the sea surface. The atmosphere influences the radar pulse, and then the signal is corrected for the ionosphere, and dry/wet troposphere effects. Besides, the altimetric measurements are corrected for known geophysical processes as solid, ocean, and pole tides, loading effect of the ocean tides, sea state bias, and the atmospheric inverse barometer (IB) response of the ocean. Detailed information of the corrections can be found at http://ctoh.legos.obs-mip.fr/.

2.2. Tide Gauge Data

In this study, revised local reference (RLR) TG data from 47 stations of the Permanent Service for Mean Sea Level (PSMSL; SPENCER and WOODWORTH, 1993) were used. Figure 1 shows the TG locations numbered from west to east along the coast, and Table 1 gives information for each TG (PSMSL code, name, latitude and longitude coordinates, and time span). In particular, we use the data from 5 TG along the Atlantic southern coast of Spain (numbers 1–5 in Table 1; Fig. 1), 41 from the northern coast of the Mediterranean (numbers 6–46), and 1 from the east coast (number 47). Data are monthly mean time series, spanning mostly from 10 to 15 years in the period 1993–2007. The southern Mediterranean coast is not studied because of the unavailability of TG measurements for the studied period.

As our primary aim is to isolate vertical crustal motion by comparing altimetric and TG measurements, the signal from both techniques should correspond to the same SLV. So, it is important to minimize possible inconsistencies due to the different corrections applied to each dataset. Thus, TG time series were corrected for several geophysical processes. Although the influence of some of the corrections in the studied trends is almost negligible, they have been included for consistency with the altimetry data. For example, the vertical displacements at the TG benchmark due to oceanic, atmospheric, and hydrological loading are corrected. The oceanic tide loading has been corrected for each TG according to the GOT4.7 tidal model (courtesy of M.S. BOS and H.-G. SCHERNECK; http://froste.oso.chalmers.se/loading/). The effects of the atmospheric and hydrological loading have been computed using
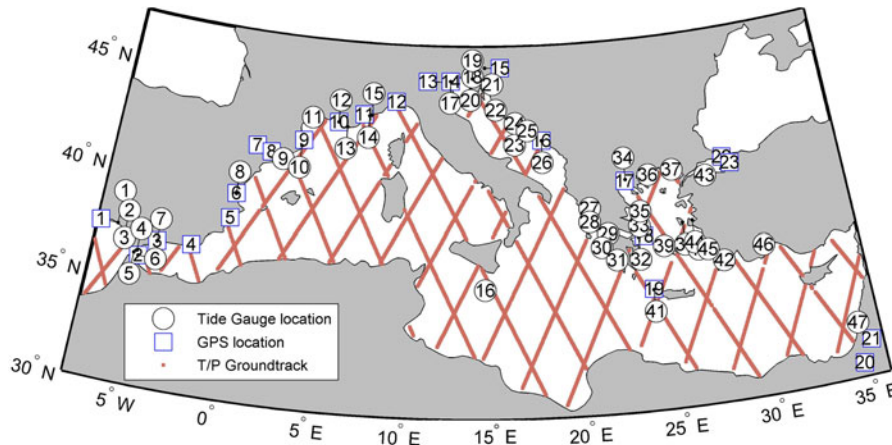
Figure 1

Data locations used in this study: (1) TG sites are represented by *numbered circles*, according to Table 1, following the coast from west to east; (2) altimeter tracks are depicted by *solid red lines*; (3) GPS sites are indicated by *blue squares* numbered according to Table 2

ECMWF reanalysis (ERA-interim; BERRISFORD *et al.*, 2009) data at the different TG locations (PETROV and BOY, 2004). In particular, the oceanic, atmospheric, and hydrological loading represent around 0.1, 2, and 2 mm, respectively, of the average standard deviation of all the TG, which is 70 mm. The addition of these corrections only accounts for around 4.3 mm, which is 6% of the signal.

The ocean and solid Earth tides are corrected with models in altimetry, which measures SLV every 10 days at the same point. The TG measures the sea level at a unique point every hour, although more recently the sampling frequency of some TG has been increased to 15 min, 6 min, and even higher rates (JOINT TECHNICAL COMMISSION for OCEANOGRAPHY and MARINE METEOROLOGY, 2006). Then, the TG time series were averaged monthly, which acts as a low-pass filter that eliminates the six largest constituents of the (ocean and solid Earth) tidal signal (CHELTON and ENFIELD, 1986). So, both datasets are corrected for these tides, and although the corrections are different, only inconsistencies at the correction error level may arise. The pole tide is corrected in altimetry following WAHR (1985), and then we apply the same correction to the TG time series. This correction accounts for 1.5 mm of the average standard deviation of all the TG, which is around 2% of the signal (DESAI, 2002). Note that this correction ignores, in both altimetry and TG, the effects of loading and self-gravitation of the ocean pole tide. The sea state bias must be corrected in

altimetry because there is only a measurement every 10 days at each point of the track. This effect is also corrected in the TG data because of the monthly averaging process mentioned above. The IB response of the ocean to atmospheric pressure changes is originally corrected in altimetry, but not in TG. As far as long-term variations are concerned, the IB effect is not important (LE TRAON and GAUZELIN, 1997). However, we decide to eliminate the IB correction in altimetry for consistency with the TG data. In any case, the trends of the altimetry minus TG time series have been computed for datasets both with and without IB correction, and they are very similar, although the error estimate is smaller when the IB correction is not applied. Therefore, after all the corrections, the TG data show the SLV, including the IB response of the ocean due to changes in the atmospheric pressure, and the signature of vertical crustal motion at the TG benchmark, such as those produced by the GIA. Although the latter is almost negligible for most sites (Table 3), it is corrected for each TG according to the ICE-5Gv1.2 (VM4) model (PELTIER, 2004).

This study is based on the fact that two independent techniques measure the SLV at a same location. However, the measurements from altimetry are made along the track of the satellite, which rarely coincides with the location of a TG (Fig. 1). So, the altimetry measurements are interpolated to each TG location. To do this, the altimetry data were convolved with a two-dimensional Gaussian function centered at the

Table 1

Information for each tide gauge. Columns from left to right correspond to: numbering as shown in Fig. 1, PSMSL station code, city and country, latitude and longitude coordinates, and span of time used in this study

No.	Code	Site	Location	Span
01	220005	Huelva (Spain)	37 08 N 06 50 W	97–06
02	220008	Bonanza (Spain)	36 48 N 06 20 W	93–07
03	220003	Cádiz III (Spain)	36 32 N 06 17 W	93–07
04	220011	Algeciras (Spain)	36 07 N 05 26 W	93–02
05	220021	Tarifa (Spain)	36 00 N 05 36 W	93–07
06	340001	Ceuta (Spain)	35 54 N 05 19 W	93–07
07	220032	Málaga II (Spain)	36 43 N 04 25 W	93–07
08	220056	Valencia (Spain)	39 28 N 00 20 W	93–05
09	220061	Barcelona (Spain)	41 21 N 02 10 E	93–07
10	220081	L'Estartit (Spain)	42 03 N 03 12 E	93–01
11	230021	Sète (France)	43 24 N 03 42 E	96–05
12	230051	Marseille (France)	43 18 N 05 21 E	93–07
13	230061	Toulon (France)	43 07 N 05 55 E	93–07
14	230081	Nice (France)	43 42 N 07 16 E	98–07
15	230011	Monaco C.	43 44 N 07 25 E	01–07
16	265001	Valletta (Malta)	35 54 N 14 31 E	00–04
17	270054	Venice P.S. (Italy)	45 26 N 12 20 E	93–00
18	270061	Trieste (Italy)	45 39 N 13 45 E	93–07
19	279003	Luka Koper (Slovenia)	45 34 N 13 45 E	93–03
20	280006	Rovinj (Croatia)	45 05 N 13 38 E	93–06
21	280011	Bakar (Croatia)	45 18 N 14 32 E	93–06
22	280013	Zadar (Croatia)	44 07 N 15 14 E	93–06
23	280021	Split RT Marjana (Croatia)	43 30 N 16 23 E	93–06
24	280031	Split Harbor (Croatia)	43 30 N 16 26 E	93–06
25	280046	Sucuraj (Croatia)	43 08 N 17 12 E	93–05
26	280081	Dubrovnik (Croatia)	42 40 N 18 04 E	93–06
27	290001	Preveza (Greece)	38 57 N 20 46 E	93–06
28	290004	Levkas (Greece)	38 50 N 20 42 E	93–06
29	290014	Patrai (Greece)	38 14 N 21 44 E	93–06
30	290017	Katakolon (Greece)	37 38 N 21 19 E	93–07
31	290021	Kalamai (Greece)	37 01 N 22 08 E	93–01
32	290030	North Salaminos (Greece)	37 57 N 23 30 E	93–00
33	290034	Khalkis North (Greece)	38 28 N 23 36 E	93–07
34	290051	Thessaloniki (Greece)	40 37 N 23 02 E	93–07
35	290037	Skopelos (Greece)	39 07 N 23 44 E	00–07
36	290061	Kavalla (Greece)	40 44 N 24 25 E	93–07
37	290065	Alexandroupoli (Greece)	40 51 N 25 53 E	93–07
38	290071	Chios (Greece)	38 23 N 26 09 E	93–07
39	290081	Siros (Greece)	37 26 N 24 55 E	98–07
40	290091	Leros (Greece)	37 05 N 26 53 E	93–07
41	290097	Soudhas (Greece)	35 30 N 24 03 E	93–01
42	290110	Rodhos (Greece)	36 26 N 28 14 E	93–07
43	310038	Erdek (Turkey)	40 23 N 27 51 E	99–04
44	310042	Mentes/İzmir (Turkey)	38 26 N 26 43 E	99–04
45	310046	Bodrum II (Turkey)	37 02 N 27 25 E	99–04
46	310052	Antalaya II (Turkey)	36 50 N 30 37 E	99–04
47	320016	Hadera (Israel)	32 28 N 34 53 E	93–07

TG location. The function takes the value 1/2 at a distance of 50 km from the TG and vanishes beyond 500 km. Altimetry data are further averaged to monthly values.

2.3. GPS Data

For comparison purposes we have included in the analysis the measurements from 23 GPS stations from the EUREF Permanent Network (EPN), which are co-located at, or close to, a TG station (Fig. 1; Table 2). Most of these GPS time series did not start until the late 1990s or early 2000s. Since the differences between altimetry and TG only give information about the vertical land motion, we only consider the GPS vertical rate of change. We use the EPN cumulative solution expressed in the global ITRF2005 reference frame (see KENYERES and BRUY-NINX 2004) as provided by EUREF. Details about the estimation procedure are available through the "Time Series Analysis" web page at the EPN Central Bureau (http://epncb.oma.be/_dataproducts/products/timeseriesanalysis/index.php)

3. Analysis and Results

SLV values in the Mediterranean present a strong seasonal signal with amplitudes of the annual cycle that range from 4 to 16 cm, explaining most of the SLV variability (VIGO et al., 2011). This is produced by both changes in the density of the water column and in the water mass budget (GARCIA-GARCIA et al., 2010). For the studied period, a model accounting for the annual, semiannual, and a linear trend was adjusted to the TG and altimetry time series using a least-squares fit to the following model:

$$\text{signal} = a + bt + A_a \sin(\omega_a t - \varphi_a) + A_{sa} \sin(\omega_{sa} t - \varphi_{sa}), \quad (1)$$

where t is time, A is amplitude, ω is frequency, φ is phase, and the subscripts "a" and "sa" refer to annual and semiannual cycles, respectively.

Then, we obtain the nonseasonal time series by subtracting all terms in this model (except for the trend one) from the original time series. After that, for each TG location, we get the difference time series for altimetry minus TG by subtracting the TG values from the geographically interpolated altimetry time series.

If all measurements were perfect and no errors were introduced by the altimetry geographical

Table 2

Vertical velocities of the EUREF GPS stations

No.	Code	Site	Location	Span	Trend	Sigma	
01	HUEL	Huelva (Spain)	37 08 N 06 50 W	07–09	−0.13	0.57	≈
02	CEU1	Ceuta (Spain)	35 54 N 05 19 W	08–09	−3.10	0.50	↓
03	MALA	Málaga (Spain)	36 43 N 04 25 W	06–09	0.43	0.34	↑
04	ALME	Almería (Spain)	36 51 N 02 28 W	01–09	−0.32	0.15	↓
05	ALAC	Alicante (Spain)	38 20 N 00 29 W	99–09	−1.47	0.16	↓
06	VALE	Valencia (Spain)	39 28 N 00 20 W	01–09	−1.26	0.23	↓
07	EBRE	Ebre (Spain)	41 49 N 00 30 E	97–09	−0.72	0.11	↓
08	BELL	Bellmunt (Spain)	41 36 N 01 24 E	99–09	−0.41	0.16	↓
09	CREU	Cap de Creus (Spain)	42 19 N 03 18 E	99–09	−0.36	0.24	↓
10	MARS	Marseille (France)	43 18 N 05 21 E	98–09	−0.99	0.25	↓
11	GRASS	Caussels (France)	43 45 N 06 55 E	96–09	0.50	0.14	↑
12	GENO	Genova (Italy)	44 25 N 08 55 E	99–09	−0.58	0.16	↓
13	PADO	Padova (Italy)	45 24 N 11 52 E	01–09	−0.67	0.19	↓
14	VENE	Venice P.S. (Italy)	45 26 N 12 20 E	02–07	−1.51	0.29	↓
15	GSR1	Geoservis GR. 1 (Slovenia)	46 03 N 14 33 E	02–09	0.04	0.24	≈
16	DUBR	Dubrovnik (Croatia)	42 40 N 18 04 E	00–09	−1.42	0.20	↓
17	AUT1	Thessaloniki (Greece)	40 37 N 23 02 E	05–09	−2.53	0.23	↓
18	NOA1	Athens (Greece)	38 00 N 23 48 E	06–09	−1.24	0.37	↓
19	TUC2	Chania (Greece)	35 32 N 24 04 E	04–09	−0.82	0.30	↓
20	RAMO	Mitzpe Ramon (Israel)	30 36 N 34 46 E	98–09	0.63	0.20	↑
21	DRAG	Metzoke Dragot (Israel)	31 36 N 35 24 E	00−09	5.08	0.38	↑
22	ISTA	Istanbul (Turkey)	41 06 N 29 01 E	00–09	1.03	0.14	↑
23	TUBI	Gebze (Turkey)	40 47 N 29 27 E	99–09	−1.89	0.14	↓

Columns from left to right correspond to: numbering shown in Fig. 1, EUREF station code, city and country, latitude and longitude coordinates, span of time, vertical velocities (mm/year), and error estimate. The last column classifies the trends as negative values (meaning land subsidence, indicated by ↓), positive values (meaning land uplift, indicated by ↑), and values indistinguishable from zero within 1 sigma (meaning no significant motion, indicated by ≈)

interpolation, SLV as measured by both TG and altimetry should be identical and thereby cancel in the altimetry minus TG time series. In this case, the remaining signal in the residuals should be produced by vertical motion at the TG location. Unfortunately, neither measurements nor procedure are perfect, and there are several source of errors, including loss of accuracy close to the coasts due to altimetry interpolation to the TG site.

Nevertheless, both datasets are remarkably consistent over their common time interval, and have close similarity in their variations of sea level at low and high frequencies. The agreement of the records provides confidence in the quality of their data. However, when examining the long-term behavior of SLV, discrepancies between the two of them arise, and these are our sought signal. As an illustration of this comparison, the time series corresponding to Marseille, Trieste, and Rovinj are depicted in the first, second, and third rows of Fig. 2, respectively. In the

left column, we present the original observation data from the two sources; in the middle one, the same signals are presented, but removing their seasonal component as described above; in the right column, we can see the respective nonseasonal altimetry minus TG time series.

Then, their linear trends are estimated by a robust multilinear regression analysis, which iteratively re-weights the least squares via a bi-square weighting function to minimize the effect of outliers in the time series. The weights are given by

$$\omega = \begin{cases} (1 - r^2)^2, & \text{if } r < 1; \\ 0, & \text{otherwise;} \end{cases} \quad \text{and}$$
$$r = \frac{e}{4{,}685 s \sqrt{1 - h}}. \tag{2}$$

In the last formula, e is the residual vector of the first iteration, h is the vector of leverage values from a least-squares fit, and s is computed as MAR/0.6745, where MAR is the median absolute residual.
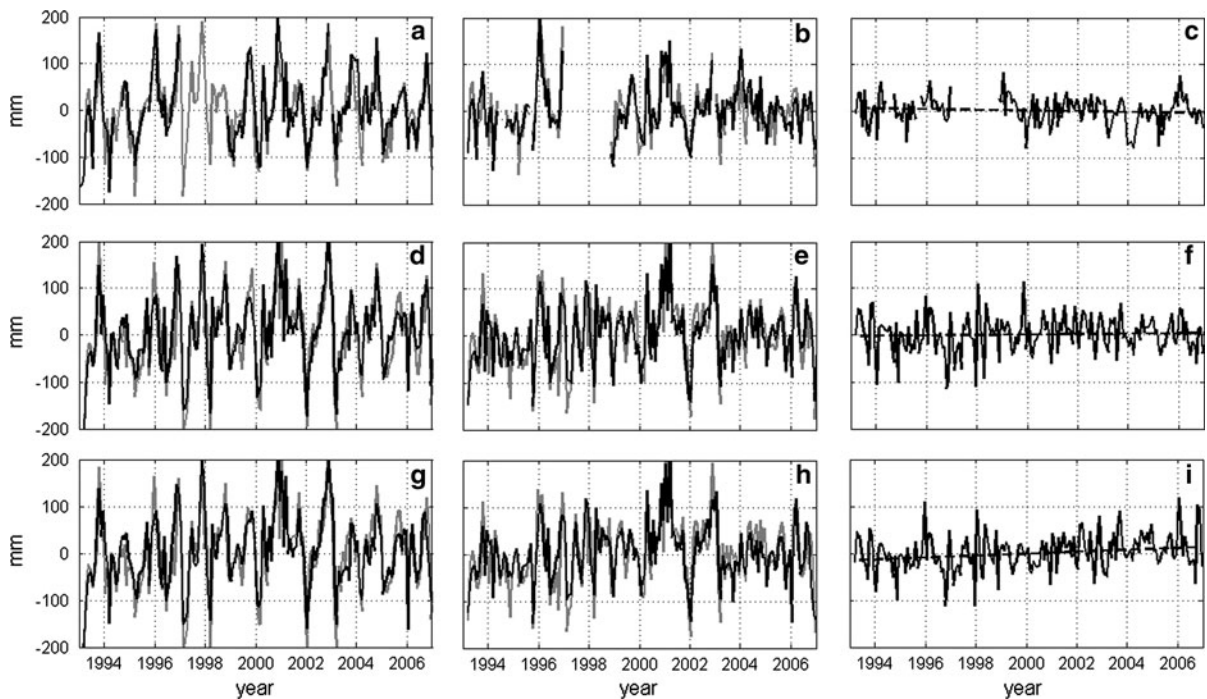
Figure 2

The *first* and *second columns* show seasonal and nonseasonal altimetry (in *black*) and TG (*grey*) time series at Marseille (*first row*), Trieste (*second row*), and Rovinj (*third row*). The *third column* shows the nonseasonal altimetry minus TG time series and its linear term. Units are mm

The resultant linear trends of the nonseasonal altimetry minus TG time series can be seen in Table 3 (column 3) and in Fig. 3. Positive linear trends represent land uplift while negative ones represent land subsidence, so Fig. 3 presents positive trends using triangles pointing up and negative ones by triangles pointing down. Circles in the figure represent trends with values indistinguishable from zero within 1 standard deviation, which account for 32% of the total TG. Table 3 also presents the GIA correction applied at each TG site, which is negligible for most of the locations.

For comparison purposes we compare our estimates of vertical crustal motion with estimates obtained from independent GPS measurements nearby the TG sites (Fig. 1). In general, their time span is shorter than that of the altimetry minus TG time series, since most of these GPS time series started in the late 1990s or early 2000s. For this reason, the period of study for both datasets does not exactly match, which can lead to differences in the estimated vertical motions. On the other hand, the

EPN cumulative solution, even though it is in the global frame, is slightly biased as it cannot perfectly reproduce the global frame (A. KENYERES and J. LEGRAND, 2009, personal communication). Moreover, the geophysical corrections applied to the GPS data are different from those used for the TG and altimetry data. Table 3 shows that the vertical motions estimated from altimetry minus TG and from GPS only agree in 4 of 13 cases. These discrepancies are in part due to the time span of the GPS time series, which is not coincident with that of the altimetry minus TG time series, or is very short. In fact, the qualitative agreement between both techniques increases to four of five cases when the linear trends are estimated for a common time span of at least 5 years (Table 4).

4. *Discussion and Conclusions*

The main objective of this work is to provide an estimation of the vertical land motion along the Mediterranean coastline from altimetry and TG sea

Table 3

Vertical velocities

TG		Altimetry minus TG (GIA corrected)	GIA correction		GPS		
No.	Site	Trend (mm/year)	ICE-5Gv1.2 (VM4) Trend (mm/year)		Station	Trend (mm/year)	
01	Huelva	−3.47 ± 1.15	−0.09	↓	HUEL	−0.13 ± 0.57	≈
02	Bonanza	−4.21 ± 0.74	−0.09	↓			
03	Cádiz III	0.25 ± 1.05	−0.07	≈			
04	Algeciras	−2.55 ± 1.69	−0.08	↓			
05	Tarifa	−4.91 ± 0.69	−0.07	↓			
06	Ceuta	0.82 ± 0.78	−0.08	↑	CEU1	−3.10 ± 0.50	↓
07	Málaga II	−3.58 ± 0.81	−0.14	↓	MALA	0.43 ± 0.34	↑
08	Valencia	−14.91 ± 1.16	−0.08	↓	VALE	−1.26 ± 0.23	↓
09	Barcelona	−5.25 ± 0.71	0.01	↓	BELL	−0.41 ± 0.15	↓
10	L'Estartit	−0.54 ± 1.18	0.01	≈	CREU	−0.36 ± 0.24	↓
11	Sète	−3.51 ± 1.18	−0.16	↓			
12	Marseille	−0.45 ± 0.62	−0.07	≈	MARS	−0.99 ± 0.25	↓
13	Toulon	−0.13 ± 0.66	−0.02	≈			
14	Nice	−3.09 ± 1.32	−0.12	↓	GRASS	0.50 ± 0.14	↑
15	Monaco C.	−5.08 ± 2.33	−0.13	↓			
16	Valletta	−6.98 ± 2.18	0.09	↓			
17	Venice P. S.	0.86 ± 2.03	−0.34	≈	VENE	−1.51 ± 0.29	↓
18	Trieste	1.10 ± 0.73	−0.34	↑			
19	Luka Koper	9.74 ± 1.64	−0.34	↑			
20	Rovinj	2.62 ± 0.77	−0.34	↑			
21	Bakar	0.89 ± 0.81	−0.34	↑			
22	Zadar	0.81 ± 1.04	−0.31	≈			
23	Split RT M	−0.49 ± 0.68	−0.29	↓			
24	Split H	−0.86 ± 0.73	−0.29	↓			
25	Sucuraj	0.59 ± 0.85	−0.29	≈			
26	Dubrovnik	−0.82 ± 0.67	−0.30	↓	DUBR	−1.42 ± 0.20	↓
27	Preveza	0.67 ± 0.88	−0.27	≈			
28	Levkas	0.64 ± 0.86	−0.25	≈			
29	Patrai	−9.17 ± 0.95	−0.25	↓			
30	Katakolon	0.09 ± 0.89	−0.17	≈			
31	Kalamai	−0.06 ± 1.79	−0.14	≈			
32	N Salaminos	9.68 ± 2.14	−0.25	↑	NOA1	−1.24 ± 0.37	↓
33	Khalkis N	−2.93 ± 0.76	−0.30	↓			
34	Thessaloniki	−0.67 ± 0.87	−0.42	↓	AUT1	−2.53 ± 0.23	↓
35	Skopelos	0.16 ± 2.43	−0.35	≈			
36	Kavalla	2.30 ± 1.93	−0.41	↑			
37	Alexandroupoli	0.12 ± 1.01	−0.40	≈			
38	Chios	0.89 ± 0.84	−0.32	↑			
39	Siros	2.48 ± 1.34	−0.19	↑			
40	Leros	4.91 ± 0.82	−0.20	↑			
41	Soudhas	5.17 ± 1.52	0.01	↑	TUC2	−0.82 ± 0.20	↓
42	Rodhos	−3.26 ± 0.72	−0.16	↓			
43	Erdek	2.45 ± 4.42	−0.42	≈			
44	Mentes/İzmir	0.16 ± 3.33	−0.36	≈			
45	Bodrum II	−12.23 ± 2.20	−0.23	↓			
46	Antalaya II	−11.90 ± 2.72	−0.33	↓			
47	Hadera	−4.72 ± 0.85	−0.22	↓			

The first column gives the TG number, and the second one the TG station name. The third column gives the linear rate of change and the formal error estimate (1 sigma) of the altimetry minus TG time series. The forth column gives the applied GIA correction. The fifth column gives the qualitative estimated motion (↑: uplift; ↓: subsidence; ≈: nonsignificant motion). The sixth, seventh, and eighth columns give, when possible, the closest GPS station from EUREF, its vertical rate, and the qualitative motion, respectively. All units are mm/year
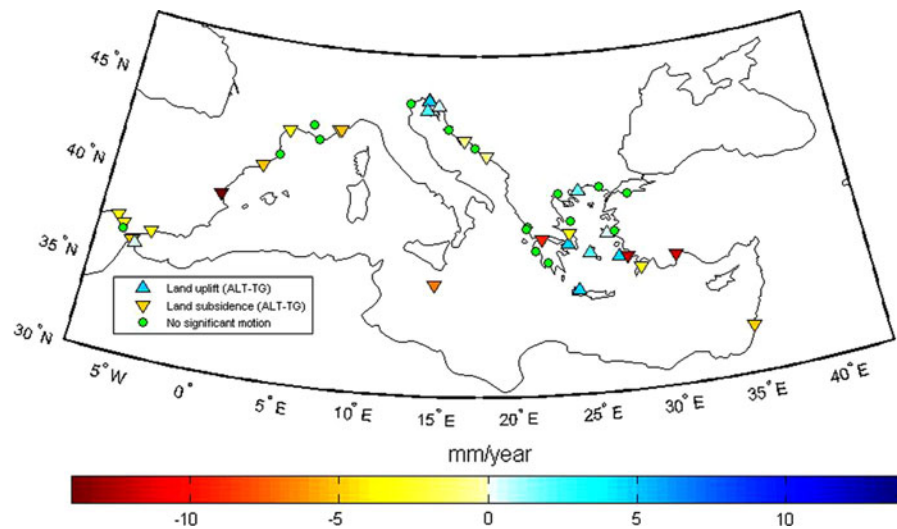
Figure 3
Colored triangles indicate the vertical land movement along the northern Mediterranean coast derived from the altimetry minus TG time series according to the third column of Table 3. *Triangles* pointing up and down represent ground uplift and subsidence, respectively. *Circles* indicate values indistinguishable from zero within 1σ

Table 4

As Table 3, but the vertical velocities are estimated in the common time span of the altimetry minus TG and the closest GPS time series

Site TG	Span	Altimetry minus TG (GIA corrected, mm/year)	GPS (mm/year)	GPS station
Valencia	01–05	-26.12 ± 3.47	-4.44 ± 0.37	VALE
Barcelona	99–07	-7.03 ± 1.41	-2.12 ± 0.14	BELL
Marseille	99–07	-0.57 ± 1.24	-3.04 ± 0.09	MARS
Nice	98–07	-3.09 ± 1.34	-0.50 ± 0.08	GRASS
Dubrovnik	01−05	-7.55 ± 2.64	-3.69 ± 0.23	DUBR

level measurements. The estimated vertical motions are potentially representative of tectonic uplift or subsidence at most of the sites. Due to the proximity to the former Alpine and Fennoscandian ice sheets, the northern Mediterranean coasts are potentially affected by the GIA (STOCCHI *et al.*, 2005). Nevertheless, GIA-related deformation of the whole basin is mainly driven by the response of the solid Earth and the geoid to loading effects of melt water since the deglaciation, which contributes to significant and widespread subsidence (STOCCHI and SPADA, 2007, 2009). In a recent work, STOCCHI and SPADA (2009) performed a comprehensive analysis with different GIA model predictions, providing upper and lower bounds on the current rate of SLV associated with GIA in the Mediterranean. The GIA-induced rate of

SLV in the eastern Mediterranean is close to zero, but at the western margin produces a falling sea level with maximum values close to −0.3 mm/year. On the other hand, the central Mediterranean is the most sensitive to GIA, reaching maximum values around 0.8 mm/year (eastern coast of Calabria and Sicily). This study accounts for the GIA correction according to PELTIER (2004), although this does not constitute a significant portion of the observed motion (Table 3). However, at quite stable sites such as Trieste (northern Italy), the GIA accounts for around 30% of the reported vertical land motion.

The results obtained in this work are in accordance with the present geodynamic framework of the Mediterranean region, whose geology has been shaped by the interplay between two plates, the

African and Eurasian ones, and smaller intervening microplates. As a result, this region is characterized by three main subsidence zones, i.e., the Alps–Betic, the Apennines–Maghrebides, and the Dinarides–Hellenides–Taurides, closely related to which are the Carpathian subsidence and the Pyrenees (see Fig. 4, modified from CARMINATI and DOGLIONI, 2004 with permission from the authors). These subsidence zones present variable rates of activity, being higher in the eastern Mediterranean and becoming quieter towards the north. However, many fundamental issues of the very complex tectonic regime of microplates remain unresolved, especially with respect to vertical motions.

Some of the present plate boundaries, especially in the eastern Mediterranean, appear to be so diffuse and so anomalous that they cannot be categorized into the three classical types of plate (boundaries-subduction, spreading, and transform). According to measurements from space-geodetic techniques, the Eurasian and African Plates converge along NW–SE direction, both rotating anticlockwise (JIMENEZ-MUNT

et al., 2003; see also NASA database on present global plate motion http://sideshow.jpl.nasa.gov/mbh/series.html). As one of the most seismotectonic active areas in Europe, the Southern Aegean and the Mediterranean ridge should be taken into special consideration. In this area, including western Turkey and Greece, many destructive earthquakes have occurred throughout history. The Island of Crete is situated on the north side of the Hellenic Arc, which is the result of the ongoing collision between the African and Eurasian Plates, with the consequent escape of the Anatolian Microplate (Turkey) sideways from the Arabia–Eurasia collision (JIMENEZ-MUNT and SABADI-NI, 2002; KREEMER and CHAMOT-ROOKE, 2004).

During the last 15 years, continuous and campaign-type GPS measurements have been used to determine the crustal motion and deformation of the eastern Mediterranean (e.g., COCARD et al., 1999; BRIOLE et al., 2000; KAHLE et al., 2000). In a recent study by HOLLENSTEIN et al. (2008) the crustal dynamics of the area of Greece and the Aegean Sea were estimated from a detailed high-quality solution
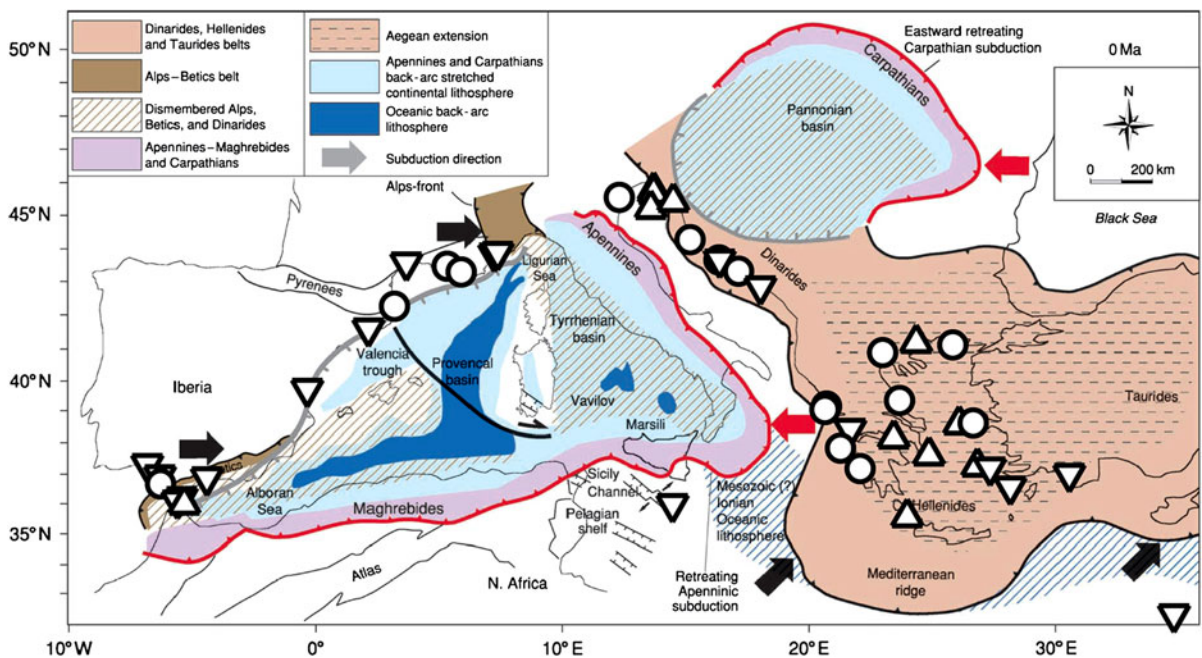

Figure 4

Geodynamic framework for the Mediterranean region as provided by CARMINATI and DOGLIONI, (2004), on which we have indicated the TG sites considered in our work as *triangles* and *circles* representing the estimated vertical motions from the altimetry minus TG time series. *Triangles* pointing up and down represent ground uplift and subsidence, respectively. *Circles* indicate values indistinguishable from zero within 1σ

based on combined processing of existing and new continuous and campaign-type GPS measurements carried out between 1993 and 2003. HOLLENSTEIN et al. (2008) have also estimated the two-dimensional dilatation rates from the strain rate fields, providing maps of crustal extension and compression of the region (see Fig. 5, modified from HOLLENSTEIN et al. 2008 with permission from the authors). In general, crustal compression has an effect of land uplift, whereas crustal extension produces land subsidence. Bearing this fact in mind, our results in the region are

in very good agreement with those provided by HOLLENSTEIN et al. (2008). Of 19 TG in the region, 9 present significant vertical motion. Of the latter, three TG presenting subsidence (numbers 29, 42, and 45) are in extension zones, three TG presenting uplift (numbers 32, 39, and 41) are in compression zones, and only three TG (numbers 36, 38, and 40) do not agree with the extension/compression zones. Among the other ten TG with values indistinguishable from zero (within 1 standard deviation), five of them (numbers 27, 28, 30, 31, and 34) are close to
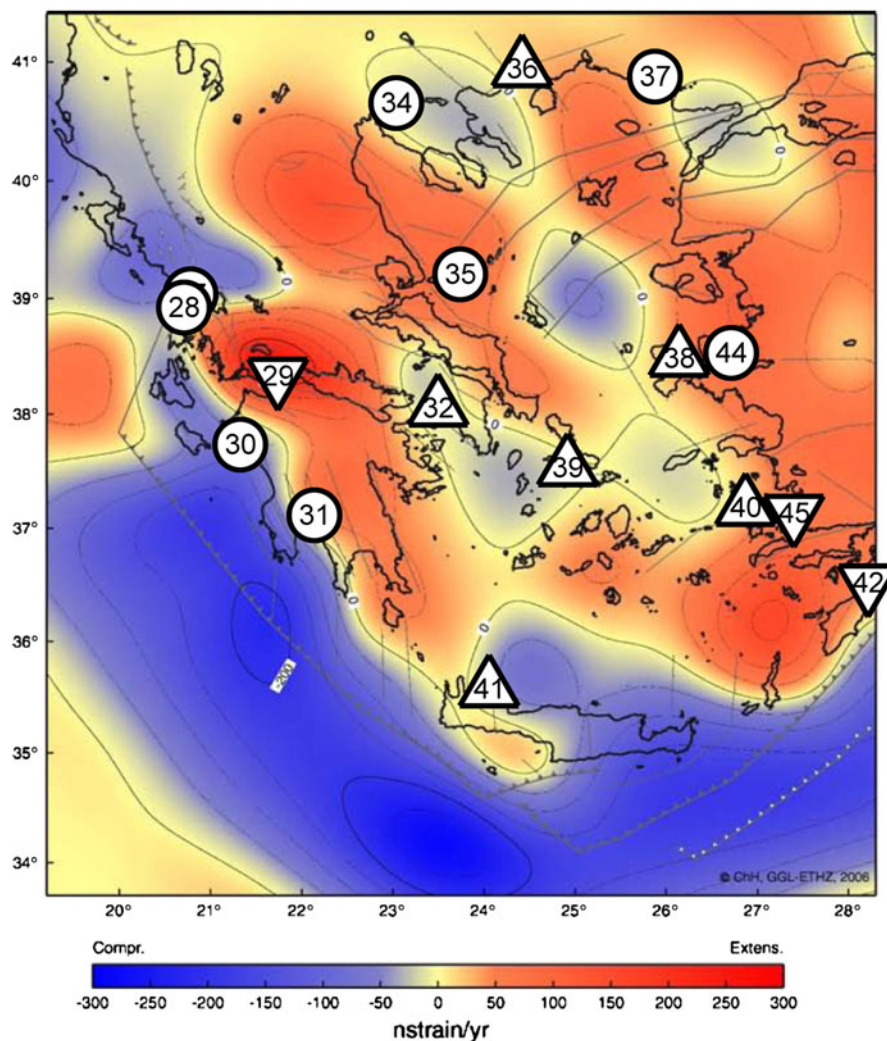
Figure 5
Crustal extension/compression map from HOLLENSTEIN et al. (2008) with qualitative estimates of the vertical crustal motion from the altimetry minus TG time series superimposed. Extension areas (representing subsidence) are shown in *red*, and compression areas (representing uplift) in *blue*. Units are number strain per year. *Numbers* correspond to TGs (Table 1). *Triangles* pointing up and down represent ground uplift and subsidence, respectively. *Circles* indicate values indistinguishable from zero (within 1σ)

transition zones from extension-compression. This remarkable consistency between both estimates for the vertical crustal displacement, in such an active region, based on completely independent techniques, provides confidence in terms of the reliability of the results. Note that the African block is subsided northward, producing uplift of the Island of Crete (RAHL *et al.*, 2004), which is in agreement with our results found at Soudhas (TG number 41).

Land movement at the coast of the Adriatic Sea is caused by the oblique contacts between the Adriatic Microplate and the Dinarides. There exist three sections of the Adriatic Microplate, differing in size and rate of movement. This results in different land movement behavior along the Dinarides zone in the northern, central, and the southern part (KUK *et al.*, 2000). Our results for the coast of the Adriatic Sea show a different land movement behavior in the northern, central, and southern part of the Dinarides zone.

It should be noted that not all the vertical crustal motion reported in this study has a geological origin; for example, Venice must be considered as a special case due to the large influence of anthropogenic effects (e.g., CARMINATI and DI DONATO, 1999). In fact, in spite of being located in a subsidence area (RUTIGLIANO *et al.*, 2000), neither this study nor BECKER *et al.* (2002) showed such subsidence. Another case is Valencia, where the altimetry minus TG time series shows an uplift of 3.2 mm/year for the period 1995–1999, which is reversed and increased by a factor of 10, reaching −29.8 mm/year, for the period 2000–2005 (Fig. 6). The origin of this abrupt change is not geology but the construction of a bridge weighing more than 2,000 tons in the Port of Valencia, close to the TG site.

In summary, in spite of several possible error sources in the altimetry minus TG time series, with a sufficiently long time span reaching 15 years, we are able to obtain estimates for the vertical ground motion at the TG sites along the northern Mediterranean Sea coast. These estimates are in agreement with independent techniques such as GPS. When no continuous GPS measurements are available, we provide new and useful information for those sites. These results provide useful source data for studying, contrasting, and constraining tectonic models of the region.
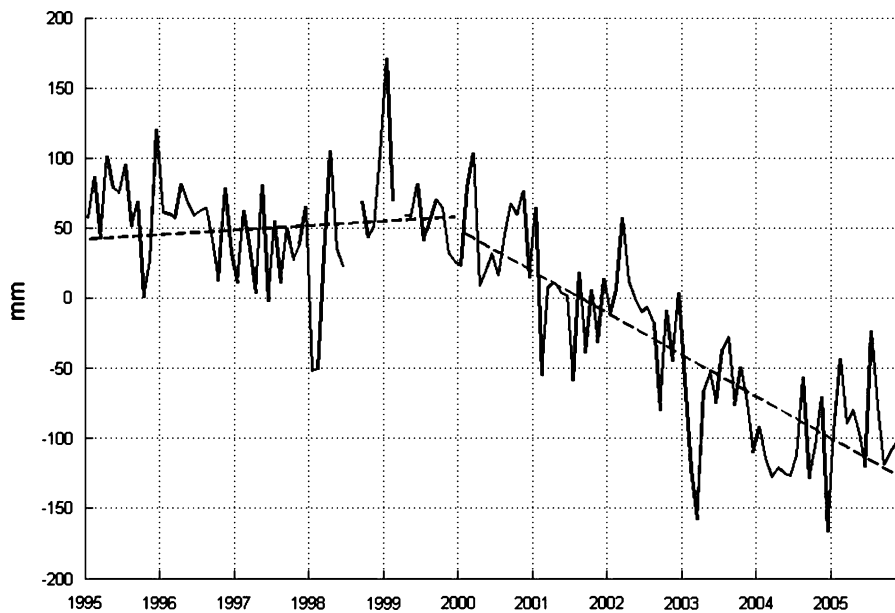

Figure 6
The *solid line* represents the altimetry minus TG time series of Valencia (east coast of Spain). *Dashed lines* represent the linear rates estimated for the periods 1995–2000 and 2000–2006, whose values are 3.2 and −29.8 mm/year, respectively

REFERENCES

BARNETT, T.P. (1984), *The Estimation of "Global" Sea Level Change: A Problem of Uniqueness*, J. Geophys. Res. 89 (C5), 7980-7988.

BECKER, M., ZERBINI, S., BAKER, T., BRKI, B., GALANIS, J., GARATE, J., GEORGIEV, I., KAHLE, H.-G., KOTZEV, V., LOBAZOV, V., MARSON, I., NEGUSINI, N., RICHTER, B., VEIS, G., and YUZEFOVICH., P. (2002), *Assessment of height variations by GPS at Mediterranean and Black Sea coast tide gauges from the SELF projects*, Global Planet. Change, *34*, 5–35.

BENNETT, R.A., HREINSDÓTTIR, S., BUBLE, B., BAI, T., BAI, E., MARJANOVI, M., CASALE, G., GENDASZEK, G., and COWAN, D. (2008), *Eocene to present subduction of southern Adria mantle lithosphere beneath the Dinarides*, Geology v. *36* no. 1 p. 3-6 doi:10.1130/G24136A.1.

BERRISFORD, P., DEE, D., FIELDING K., FUENTES, M., KAALLERG, P., KOBAYASHI, S., and UPPALA, S.M. (2009), *The ERA-Interim Archive*, Tech rep., ERA Report Series No 1.

BRIOLE P., RIGO A., LYON-CAEN H., RUEGG J.C., PAPAZISSI K., MITSAKAKI C., BALODIMOU A., VEIS G., HATZFELD D., and DESCHAMPS A. (2000), *Active deformation of the Corinth rift, Greece: Results from repeated Global Positioning System surveys between 1990 and 1995*: J. Geophys. Res. *105* (25), 605-625.

CARMINATI, E., and DI DONATO, G. (1999), *Separating natural and anthropogenic vertical movements in fast subsiding areas: The Po Plain (N. Italy) Case*, Geophys. Res. Lett., *26* (15), 2291–2294.

CARMINATI, E., and DOGLIONI, C. Mediterranean tectonics. Encyclopedia of Geology (Elsevier, 2004).

CAZENAVE, A., DOMINH, K., PONCHAUT, F., SOUDARIN, L., CRETAUX, J.F., and LE PROVOST, C. (1999), *Sea level changes from Topex-Poseidon altimetry and tide gauges, and vertical crustal motions from DORIS*. Geophys. Res. Lett., *26*, 2077-2080.

CHELTON, D.B., and ENFIELD, D.B. (1986), *Ocean Signals in Tide Gauge Records*, J. Geophys. Res. *91* (B9), 9081-9098.

COCARD, M., KAHLE, H.G., PETER, Y. GEIGER, A., VEIS, G., FELEKIS, S., PARADISIS, D. and BILLIRIS, H. (1999), *New constraints on the rapid crustal motion of the Aegean region: recent results inferred from GPS measurements (1993-1998) across the West Hellenic Arc, Greece*, Earth Planet. Sci. Lett., *172*, 39-47.

DESAI, S.D. (2002), *Observing the pole tide with satellite altimetry*, J. Geophys. Res., *107*(C11), 3186, doi:10.1029/2001JC001224.

DOUGLAS, B.C. (1991), *Global Sea Level Rise*, J. Geophys. Res., *96* (C4), 6981–6992.

GARCIA, D., VIGO, I., CHAO, B.F. and MARTÍNEZ, M.C. (2007), *Vertical Crustal Motion along the Mediterranean and Black Sea Coast Derived from Ocean Altimetry and Tide Gauge Data*, Pure Appl. Geophys. 164, 851–863.

GARCIA-GARCIA, D., CHAO, B.F., and BOY, J.-P. (2010), *Steric and Mass-Induced Sea Level Variations in the Mediterranean Sea, Revisited*, J. Geophys. Res., in press, doi:10.1029/2009JC005928.

HOLLENSTEIN, C.H., MÜLLER, M.D., GEIGER, A., and KAHLE, H.G. (2008), *Crustal motion and deformation in Greece from a decade of GPS measurements, 1993–2003*, Tectonophysics 449, 17–40.

JOINT TECHNICAL COMMISSION FOR OCEANOGRAPHY and MARINE METEOROLOGY (2006), Manual on Sea Level Measurement and Interpretation Volume IV: An Update to 2006. Technical Report No. 31WMO/TD. No. 1339. http://www.jcomm.info/.

JIMENEZ-MUNT, I., and SABADINI, R. (2002), *The block-like behavior of Anatolia envisaged in the modeled and geodetic strain rates*, Geophys. Res. Lett. 29 (20), 1978, doi:10.1029/2002GL015995.

JIMENEZ-MUNT, I., SABADINI, R., GARDI, A., and BIANCO, G. (2003), *Active deformation in the Mediterranean from Gibraltar to Anatolia inferred from numerical modeling and geodetic and seismological data*, J. Geophys. Res., *108*(B1), 2006, doi:10.1029/2001JB001544.

KAHLE, H.-G., COCARD, M., PETER, Y., GEIGER, A., REILINGER, R., BARKA, A., and VEIS, G. (2000), *GPS-derived strain rate field within the boundary zones of Eurasian, African, and Arabian plates*, J. Geophys. Res., 105 (23), 23353-23370.

KENYERES, A., and BRUYNINX, C. (2004), Monitoring of the EPN Coordinate Time Series for Improved Reference Frame Maintenance GPS solutions, Vol 8, No 4, 200-209.

KREEMER, C., and CHAMOT-ROOKE, N. (2004), *Contemporary kinematics of the southern Aegean and the Mediterranean Ridge*. Geophysical Journal International, v. *157*, no. 3, pp 1377–1392.

KUK, V., PRELOGOVIC, E., and DRAGICEVIC, I. (2000), *Seismotectonically Active Zones in the Dinarides*. Geol. Croat., *53/2*, 295-303.

LE TRAON, P., and GAUZELIN, P. (1997), *Response of the Mediterranean mean sea level to atmospheric pressure forcing*, J. Geophys. Res., *102*(C1), 973–984.

PELTIER W.R. (2004), *Global Glacial Isostasy and the Surface of the Ice-Age Earth: The ICE-5G(VM2) model and GRACE*, Ann. Rev. Earth Planet. Sci., *32*, 111-149.

PETROV L., and BOY, J.-P. (2004) *Study of the atmospheric pressure loading signal in VLBI observations*, J. Geophys. Res., Vol. *109*, No. B03405. doi:10.1029/2003JB002500.

RAHL, J. M., FASSOULAS, C., and BRANDON, M.T. (2004), Exhumation of high-pressure metamorphic rocks within an active convergent margin, Crete, Greece: A field guide, 32th International Geological Congress, Vol. 2 – from B16 to B33, art. No B32.

RAY, R.D., BECKLEY, B.D., and LEMOINE, F.G. (2010), *Vertical crustal motion derived from satellite altimetry and tide gauges, and comparisons with DORIS measurements*, Adv. Space Res., *45*, 1510–1522.

RUTIGLIANO, P., FERRARO, C., DEVOTI, R., LANOTTE, R., LUCERI, V., NARDI, A., PACIONE, R., and SCIARRETTA, C. (2000), Vertical motions in the Western Mediterranean area from geodetic and geological data, in the proceedings of The Tenth General Assembly of the Wegener Project.

SPENCER, N.E., and WOODWORTH, P.L. (1993), Data Holdings of the Permanent Service for Mean Sea Level, Bidston, Birkenhead: Permanent Service for Mean Sea Level. 81.

STOCCHI, P., SPADA, G. and CIANETTI, S. (2005), *Isostatic rebound following the Alpine deglaciation: impact on the sea level variations and vertical movements in the Mediterranean region*, Geophys. J. Int., *162*, doi:10.1111/j.1365-246X.2005.02653.x.

STOCCHI, P., and SPADA, G.(2007), *Glacio and hydro-isostasy in the Mediterranean Sea: Clark's zones and role of remote ice sheets*, Ann. Geophys., *50* (6), 741–761.

STOCCHI P., and SPADA, G. (2009), *Influence of glacial isostatic adjustment upon current sea level variations in the Mediterranean*. Tectonophysics, *474*, 56–68.

VIGO, M.I., SÁNCHEZ-REALES, J.M., TROTTINI, M., and CHAO B.F., *Mediterranean Sea level variations: Analysis of the satellite altimetric data, 1992–2008*. J. GEODYN. (2011), doi:10.1016/j.jog.2011.02.00).

WAHR, J.W. (1985), *Deformation Induced by Polar Motion*, J. Geophys. Res., *90* (B11), 9363–9368.